Origins of Selectivity in Molecular and Supramolecular Entities: Solvent and Electrostatic Control of the Translational Isomerism in [2]Catenanes†

Françisco M. Raymo, K. N. Houk,* and J. Fraser Stoddart*

Department of Chemistry and Biochemistry, University of California, 405 Hilgard Avenue, Los Angeles, California 90095-1569

Received March 24, 1998

The fundamental basis for the stabilization of molecular complexes of various dioxyarenes and/or dithiaarenes and a tetracationic cyclophane was established by empirical force field and ab initio quantum mechanical calculations. The more stable translational isomers of the related [2]catenanes do not necessarily correspond to the more stable complexes involving the individual components. The origin of this anomaly was investigated using the AMBER* force field. Each [2]catenane is composed of cyclobis(paraquat-*p*-phenylene)—the tetracationic cyclophane—and one constitutionally unsymmetrical macrocyclic polyether, incorporating 1,4-dioxybenzene and a dioxyarene or a dithiaarene unit as its two π-electron rich recognition sites. The calculated and experimental isomer ratios at equilibrium for these [2]catenanes are in good agreement. In two instances, the calculated ratios invert as a result of changing the solvation model from H_2O to $CHCl_3$. There is a correlation between the experimental and theoretical observations for the equilibrated isomer ratios and the dielectric constant of the solvent. Both the solvation energies of the translational isomers and the energy differences associated with the corresponding complexes govern the nature of the translational isomerism. The relative stabilities of isomers are controlled by the electrostatic potential at the surface of the π-electron rich aromatic units, rather than by charge-transfer interactions.

Introduction

The self-assembly of [2]catenanes,[1,2] such as **1** (Figure 1),[3] provides a new entry to mechanically interlocked molecules. These *molecular* compounds incorporate the π-electron deficient bipyridinium-based cyclophane, cyclobis(paraquat-*p*-phenylene), and one π-electron rich dioxyarene- and/or dithiaarene-based macrocyclic polyether. Cooperative noncovalent bonding interactions, such as $\pi-\pi$ stacking,[4] [CH···O],[5] and [CH···π] interactions,[6] between the complementary recognition sites may contribute to these self-assembly processes.[7] The quantitative understanding of how self-assembly processes are controlled is one of the major frontiers of supramolecular chemistry. The electrochemical and photochemical properties of these [2]catenanes suggest that charge transfer

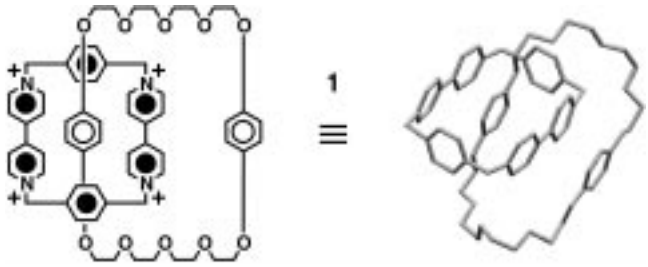

Figure 1. The symmetrical [2]catenane **1** and a polytube representation of its solid-state geometry.

* Fax: (310) 206 1843. E-mail: houk@chem.ucla.edu. E-mail: stoddart@chem.ucla.edu.

† Molecular Meccano. 28. For part 27, see: Ashton, P. R.; Matthews, O. A.; Menzer, S.; Raymo, F. M.; Spencer, N.; Stoddart, J. F.; Williams, D. J. *Liebigs Ann./Recl.* **1997**, 2485−2494.

(1) For accounts and reviews on self-assembling approaches to [2]-catenanes, based on $\pi-\pi$ stacking interactions, see: (a) Philp, D.; Stoddart, J. F. *Synlett* **1991**, 445−458. (b) Amabilino, D. B.; Stoddart, J. F. *Pure Appl. Chem.* **1993**, *65*, 2351−2359. (c) Pasini, D.; Raymo, F. M.; Stoddart, J. F. *Gazz. Chim. Ital.* **1995**, *125*, 431−443. (d) Amabilino, D. B.; Raymo, F. M.; Stoddart, J. F. *Comprehensive Supramolecular Chemistry*, Vol. 9; Hosseini, M. W., Sauvage, J.-P., Eds.; Pergamon Press: Cambridge, **1996**; pp 85−130. (e) Gillard, R. E.; Raymo, F. M.; Stoddart, J. F. *Chem. Eur. J.* **1997**, *3*, 1933−1940.

(2) For accounts and reviews on catenanes, see: (a) Schill, G. *Catenanes, Rotaxanes and Knots*; Academic Press: New York, 1971. (b) Walba, D. M. *Tetrahedron* **1985**, *41*, 3161−3212. (c) Dietrich-Buchecker, C. O.; Sauvage, J.-P. *Chem. Rev.* **1987**, *87*, 795−810. (d) Dietrich-Buchecker, C. O.; Sauvage J.-P. *Bioorg. Chem. Front.* **1991**, *2*, 195−248. (e) Chambron, J.-C.; Dietrich-Buchecker, C. O.; Sauvage, J.-P. *Top. Curr. Chem.* **1993**, *165*, 131−162. (f) Amabilino, D. B.; Stoddart, J. F. *Chem. Rev.* **1995**, *95*, 2725−2828. (g) Belohradsky, M.; Raymo, F. M.; Stoddart, J. F. *Collect. Czech. Chem. Commun.* **1996**, *61*, 1−43; **1997**, *62*, 527−557.

(3) For the synthesis and properties of the [2]catenane **1**, see: (a) Ashton, P. R.; Goodnow, T. T.; Kaifer, A. E.; Reddington, M. V.; Slawin, A. M. Z.; Spencer, N.; Stoddart, J. F.; Vicent, C.; Williams, D. J. *Angew. Chem., Int. Ed. Engl.* **1989**, *28*, 1396−1399. (b) Anelli, P. L.; Ashton, P. R.; Ballardini, R.; Balzani, V.; Delgado, M.; Gandolfi, M. T.; Goodnow, T. T.; Kaifer, A. E.; Philp, D.; Pietraszkiewicz, M.; Prodi, L.; Reddington, M. V.; Slawin, A. M. Z.; Spencer, N.; Stoddart, J. F.; Vicent, C.; Williams, D. J. *J. Am. Chem. Soc.* **1992**, *114*, 193-218.

(4) In these [2]catenanes, $\pi-\pi$ stacking interactions between the complementary π-electron deficient bipyridinium units and π-electron rich dioxyarene and/or dithiaarene units are observed. For accounts and reviews on $\pi-\pi$ stacking interactions, see: (a) Schwartz, M. H. *J. Inclusion Phenom.* **1990**, *9*, 1−35. (b) Hunter, C. A.; Sanders, J. K. M. *J. Am. Chem. Soc.* **1990**, *112*, 5525−5534. (c) Schneider, H.-J. *Angew. Chem., Int. Ed. Engl.* **1991**, *30*, 1417−1436. (d) Cozzi, F.; Cinquini, M.; Annunziata, R.; Dwyer, T.; Siegel, J. S. *J. Am. Chem. Soc.* **1992**, *114*, 5729−5733. (e) Williams, J. H. *Acc. Chem. Res.* **1993**, *26*, 593−598. (f) Hunter, C. A. *Angew. Chem., Int. Ed. Engl.* **1993**, *32*, 1584−1586. (g) Cozzi, F.; Cinquini, M.; Annunziata, R.; Siegel, J. S. *J. Am. Chem. Soc.* **1993**, *115*, 5330−5331. (h) Hunter, C. A. *J. Mol. Biol.* **1993**, *230*, 1025−1054, (i) Dahl, T. *Acta Chem. Scand.* **1994**, *48*, 95−116. (j) Cozzi, F.; Siegel, J. S. *Pure Appl. Chem.* **1995**, *67*, 683−689. (k) Shetty, A. S.; Zhang, J.; Moore, J. S. *J. Am. Chem. Soc.* **1996**, *118*, 1019−1027. (l) Hirsch, K. A.; Wilson, S. R.; Moore, J. S. *Chem. Eur. J.* **1997**, *3*, 765−771.

S0022-3263(98)00543-X CCC: $15.00
Published on Web 08/29/1998

between the aromatic donors and the bipyridinium acceptors may be significant. The separate macrocyclic components are colorless, but the [2]catenanes show[3] strong absorption bands centered between 460 and 560 nm, arising from charge-transfer interactions between the π-electron deficient bipyridinium units and the π-electron rich dioxyarene and/or dithiaarene units. Furthermore, the redox potentials associated with the reversible reduction of the two bipyridinium units are shifted[3] significantly to more negative values upon converting the "free" cyclobis(paraquat-*p*-phenylene) to the mechanically interlocked [2]catenanes. This change can be ascribed to the $\pi-\pi$ stacking interactions sustained by these units and the dioxyarene and/or dithiaarene π-donors. The contribution of charge transfer to the overall $\pi-\pi$ stacking interactions has been a matter of considerable discussion.[8] While electrostatic interactions correlate with the geometries of binding,[4b,h] little is known about how binding energies are influenced. To understand what controls the self-assembly of supramolecular entities, we must understand the relative contribution of various forces. The existence of translational isomerism in the [2]catenanes provides an outstanding opportunity to quantify these factors.

The rates of the dynamic processes associated with the [2]catenane **1** in solution are governed[3] by the noncovalent bonding interactions between the components. In particular, the circumrotation—i.e., a local *translation*—of the macrocyclic polyether through the cavity of the tetracationic cyclophane exchanges (Figure 2) the "inside" and "alongside" 1,4-dioxybenzene units, leading to the equilibration between two degenerate states. When **A** and **B** in Figure 2 are different, the two states become *translational isomers*.[9] The ratio between the two translational isomers is controlled by the noncovalent bonding interactions occurring between the aromatic unit inserted inside the cavity of the tetracationic cyclophane component and the sandwiching bipyridinium units. The relative stabilities (Figure 2) of the model *supramolecular* complexes are expected to be related to the stabilities of the two translational isomers of the corresponding [2]catenane.

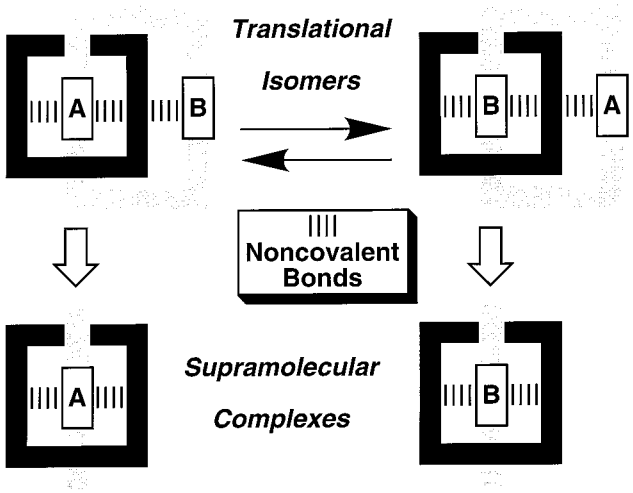

Figure 2. Translational isomers associated with an unsymmetrical [2]catenane and their corresponding supramolecular complexes.

More than 40 [2]catenanes incorporating unsymmetrical macrocyclic polyethers have been self-assembled.[10] Where single crystal X-ray analyses have been performed, only one of the two possible translational isomers has been observed. In solution, however, the ratio between the two translational isomers ranges from 50:50 up to 100:0, as revealed by ^{1}H NMR spectroscopy. This ratio is solvent[10a] or temperature[10g] dependent in some

(5) In these [2]catenanes, [CH···O] hydrogen bonding interactions between the acidic bipyridinium hydrogen atoms and the polyether oxygen atoms are observed. For accounts and reviews on hydrogen bonding interactions, see: (a) Etter, M. *Acc. Chem. Res.* **1990**, *23*, 120−126. (b) Etter, M. C.; MacDonald, J. C.; Bernstein, J. *Acta Crystallogr.* **1990**, *B46*, 256−262. (c) Rebek, J., Jr. *Angew. Chem., Int. Ed. Engl.* **1990**, *29*, 245−255. (d) Hamilton, A. D. *J. Chem. Educ.* **1990**, *67*, 821−828. (e) Desiraju, G. R. *Acc. Chem. Res.* **1991**, *24*, 290−296. (f) Aakeröy, C. B.; Seddon, K. R. *Chem. Soc. Rev.* **1993**, *22*, 397−407. (g) MacDonald, J. C.; Whitesides, G. M. *Chem. Rev.* **1994**, *94*, 2383−2420. (h) Lehn, J. M. *Pure Appl. Chem.* **1994**, *66*, 1961−1966. (i) Bernstein, J.; Davis, R. E.; Shimoni, L.; Chang, N. L. *Angew. Chem., Int. Ed. Engl.* **1995**, *34*, 1555−1573. (j) Burrows, A. D.; Chan, C. W.; Chowdhry, M. M.; McGrady, J. E.; Mingos, D. M. P. *Chem. Soc. Rev.* **1995**, *24*, 329−339. (k) Platts, J. A.; Howard, S. T.; Bracke, B. R. F. *J. Am. Chem. Soc.* **1996**, *118*, 2726−2733. (l) Desiraju, G. R. *Chem. Commun.* **1997**, 1475−1482.

(6) In these [2]catenanes, [CH···π] edge-to-face T-type interactions between the hydrogen atoms attached to the π-electron rich dioxyarene or dithiaarene units and the π-surfaces of the *p*-xylene spacers incorporated within the tetracationic cyclophane component are observed. For accounts and reviews on edge-to-face T-type interactions, see: (a) Nishio, M.; Hirota, M. *Tetrahedron* **1989**, *45*, 7201−7245. (b) Oki, M. *Acc. Chem. Res.* **1990**, *23*, 351−356. (c) Jorgensen, W. L.; Severance, D. L. *J. Am. Chem. Soc.* **1990**, *112*, 4768−4774. (d) Etter, M. C. *J. Phys. Chem.* **1991**, *95*, 4601−4610. (e) Zaworotko, M. J. *Chem. Soc. Rev.* **1994**, *23*, 283−288. (f) Nishio, M.; Umezawa, Y.; Hirota, M.; Takeuchi, Y. *Tetrahedron* **1995**, *51*, 8665−8701.

(7) For accounts and reviews on self-assembly processes, see: (a) Stoddart, J. F. In *Chirality in Drug Design and Synthesis*; Brown, C., Ed.; Academic Press: London, 1990; pp 53−81. (b) Mallouk, T. E.; Lee, H. *J. Chem. Educ.* **1990**, *67*, 829−834. (c) Constable, E. C. *Angew. Chem., Int. Ed. Engl.* **1991**, *30*, 1450−1451. (d) Lindsey, J. S. *New J. Chem.* **1991**, *15*, 153−180. (e) Whitesides, G. M.; Mathias, J. P.; Seto, C. T. *Science* **1991**, *254*, 1312−1319. (f) Whitesides, G. M.; Simanek, E. E.; Mathias, J. P.; Seto, C. T.; Chin, D. N.; Mammen, M.; Gordon, D. M. *Acc. Chem. Res.* **1995**, *25*, 37−44. (g) Menger, F. M.; Lee, S. S.; Tao, X. *Adv. Mater.* **1995**, *7*, 669−671. (h) Ghadiri, M. R. *Adv. Mater.* **1995**, *7*, 675−677. (i) Hunter, C. A. *Angew. Chem., Int. Ed. Engl.* **1995**, *34*, 1079−1081. (l) Lawrence, D. S.; Jiang, T.; Levett, M. *Chem. Rev.* **1995**, *95*, 2229−2260. (m) Raymo, F. M.; Stoddart, J. F. *Curr. Opin. Coll. Interface Sci.* **1996**, *1*, 116−126. (n) Philp, D.; Stoddart J. F. *Angew. Chem., Int. Ed. Engl.* **1996**, *35*, 1154−1196. (o) Fyfe, M. C. T.; Stoddart, J. F. *Acc. Chem. Res.* **1997**, *30*, 393−401.

(8) For a discussion on the role of charge-transfer interactions in donor−acceptor complexes, see ref 4b and Morokuma, K. *Acc. Chem. Res.* **1977**, *10*, 294−300.

(9) The term *translational isomerism* was first proposed by Schill, see: (a) Schill, G.; Rissler, K.; Fritz, H.; Vetter, W. *Angew. Chem., Int. Ed. Engl.* **1981**, *20*, 187−189. Several translationally isomeric catenanes (ref 10) and rotaxanes have been self-assembled by us. For examples of translationally isomeric rotaxanes, see: (b) Anelli, P.-L.; Asakawa, M.; Ashton, P. R.; Bissel, R. A.; Clavier, G.; Górski, R.; Kaifer, A. E.; Langford, S. J.; Mattersteig, G.; Menzer, S.; Philp, D.; Slawin, A. M. Z.; Spencer, N.; Stoddart, J. F.; Tolley, M. S.; Williams, D. J. *Chem. Eur. J.*, **1997**, *3*, 1113−1135 and references therein.

(10) (a) Ashton, P. R.; Blower, M.; Philp, D.; Spencer, N.; Stoddart, J. F.; Tolley, M. S.; Ballardini, R.; Ciano, M.; Balzani, V.; Gandolfi, M. T.; Prodi, L.; McLean, C. H. *New J. Chem.* **1993**, *17*, 689−695. (b) Amabilino, D. B.; Ashton, P. R.; Brown, G. R.; Hayes, W.; Stoddart, J. F.; Tolley, M. S.; Williams, D. J. *J. Chem. Soc., Chem. Commun.* **1994**, 2479−2482. (c) Amabilino, D. B.; Anelli, P. L.; Ashton, P. R.; Brown, G. R.; Córdova, E.; Godínez, L. A.; Hayes, W.; Kaifer, A. E.; Philp, D.; Slawin, A. M. Z.; Spencer, N.; Stoddart, J. F.; Tolley, M. S.; Williams, D. J. *J. Am. Chem. Soc.* **1995**, *117*, 11142−11170. (d) Ashton, P. R.; Huff, J.; Menzer, S.; Parsons, I. W.; Preece, J. P.; Stoddart, J. F.; Tolley, M. S.; White, A. J. P.; Williams, D. J. *Chem. Eur. J.* **1996**, *2*, 31−44. (e) Gillard, R. E.; Stoddart, J. F.; White, A. J. P.; Williams, B. J.; Williams, D. J. *J. Org. Chem.* **1996**, *61*, 4504−4505. (f) Asakawa, M.; Ashton, P. R.; Boyd, S. E.; Brown, C. L.; Gillard, R. E.; Kocian, O.; Raymo, F. M.; Stoddart, J. F.; Tolley, M. S.; White, A. J. P.; Williams, D. J. *J. Org. Chem.* **1997**, *62*, 26−37. (g) Asakawa, M.; Ashton, P. R.; Dehaen, W.; L'Abbé, G.; Menzer, S.; Nouwen, J.; Raymo, F. M.; Stoddart, J. F.; Tolley, M. S.; Toppet, S.; White, A. J. P.; Williams, D. J. *Chem. Eur. J.* **1997**, *3*, 772−787. (h) Ballardini, R.; Balzani, V.; Credi, A.; Brown, C. L., Gillard, R. E., Montalti, M., Philp, D., Stoddart, J. F., Venturi, M.; White, A. J. P.; Williams, B. J.; Williams, D. J. *J. Am. Chem. Soc.* **1997**, *119*, 12503−12513.

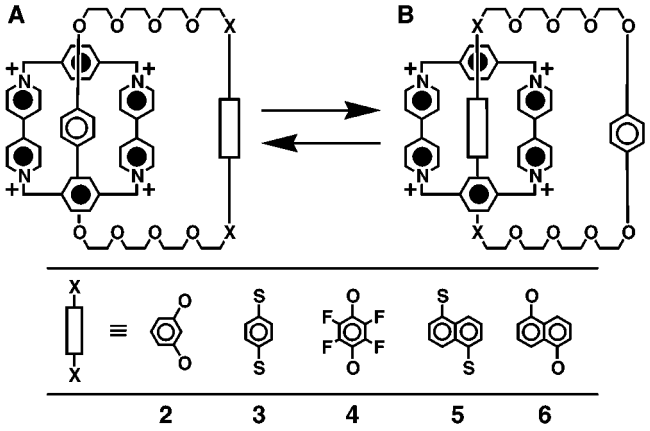

Figure 3. Translational isomerism associated with the unsymmetrical [2]catenanes **2**−**6**.

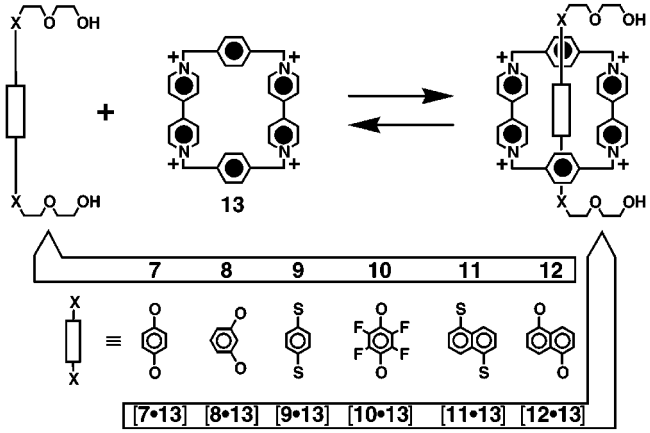

Figure 4. Complexation of the acyclic polyethers **7**−**12** by the tetracationic cyclophane **13**.

instances. To our surprise, the ratio between the translational isomers is not directly related to the binding energies of the corresponding supramolecular complexes. In order to understand (i) the factors governing the equilibrium proportions of the translational isomers, (ii) why analogous supramolecular complexes show different stabilities, and (iii) the nature of the $\pi-\pi$ stacking interactions associated with these systems, we have performed a computational investigation on the five unsymmetrical [2]catenanes **2**−**6** (Figure 3) and on their model supramolecular complexes [**7**•**13**]−[**12**•**13**] (Figure 4). These [2]catenanes incorporate a bipyridinium-based tetracationic cyclophane and macrocyclic polyethers which differ in the nature and/or substitution pattern of one of their two π-electron rich recognition sites. The model

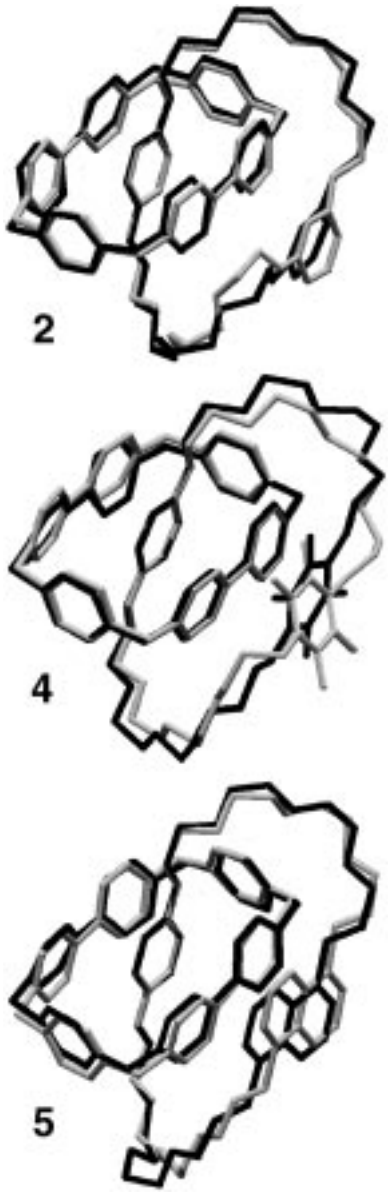

Figure 5. Sumperimposed calculated (black) and solid state (grey) geometries of the unsymmetrical [2]catenanes **2**, **4**, and **5**.

complexes incorporate the same bipyridinium-based tetracationic cyclophane and acyclic dioxyarene- or dithiaarene-based polyethers.

Results and Discussion

Method. Each complex (Figure 4) and its two separate components were subjected[11] individually to Monte Carlo conformational searches[12] employing the AMBER* force field[13] and the generalized-Born surface area (GB/SA) solvation model[14] for H_2O as implemented in Macromodel 5.0.[15] The energy differences ΔE [$\Delta E = E_{complex} - (E_{host} + E_{guest})$] between the energies of the global minima found for each complex ($E_{complex}$) and the sum of the energies of the global minima found for its two separate host (E_{host}) and guest (E_{guest}) components are listed in Table 1. To analyze the origin of the differences in ΔE values, the

(11) The separate host and guest were constructed within the input mode of Macromodel 5.0, and their geometries were optimized by energy minimization with the AMBER* force field and the GB/SA solvation model for H_2O. The resulting structures were subjected individually to Monte Carlo conformational searches. The complexes were constructed manually by docking the energy-minimized structure of the guest inside the cavity of the energy-minimized structure of the host. Then, the resulting geometries were subjected individually to Monte Carlo conformational searches as described for the separate host and guest.

(12) Chang, G.; Guida, W. C.; Still, W. C. *J. Am. Chem. Soc.* **1989**, *111*, 4379−4386.

(13) Weiner, S. J.; Kollman, P. A.; Case, D. A.; Singh, V. C.; Ghio, C.; Alagona, G.; Profeta, S., Jr; Weiner, P. *J. Am. Chem. Soc.* **1984**, *106*, 765−784.

(14) Still, W. C.; Tempczyk, A.; Hawley, R. C.; Hendrckson, T. *J. Am. Chem. Soc.* **1990**, *112*, 6127−6129.

(15) Mahamadi, F.; Richards, N. G. K.; Guida, W. C.; Liskamp, R.; Lipton, M.; Caufield, D.; Chang, G.; Hendrickson, T.; Still, W. C. *J. Comput. Chem.* **1990**, *11*, 440−467.

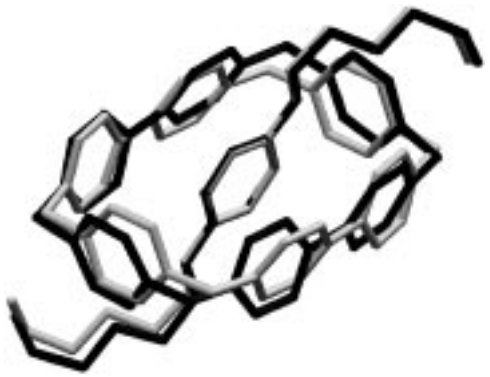

Figure 6. Superimposed calculated (black) and solid state (grey) geometries of the complex [**7**·**13**].

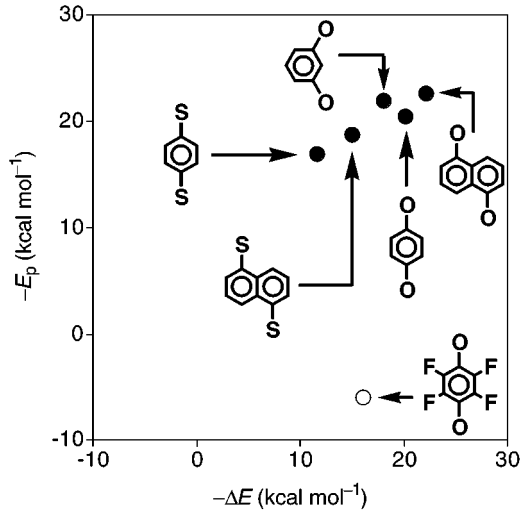

Figure 7. Correlation between the electrostatic potential E_p calculated on the surface of the aromatic units of dioxyarene and dithiaarene model compounds analogous to the guests **7**−**12**, but bearing methoxy instead of polyether substituents, and the energy differences ΔE calculated for the complexes [**7**·**13**]−[**12**·**13**].

electrostatic potential[16] E_p calculated on the surface of the aromatic units, as well as the energies of the highest occupied molecular orbitals (HOMO) E_{HOMO} associated with dioxyarene and dithiaarene compounds analogous to **7**−**12** but bearing methoxy substituents instead of the polyether chains, were determined[17,18] by single point ab initio calculations performed at the HF/6-31G** level without including solvent effects.

The translational isomers **A** and **B** of each [2]catenane (Figure 3) were subjected[19] individually to a Monte Carlo conformational search, employing the AMBER* force field and the GB/SA solvation model for H_2O and $CHCl_3$, in separate runs, as implemented in Macromodel 5.0. The energies E(**A**) and E(**B**) associated with the global minima found for the translational isomers **A** and **B**, respectively, of each [2]catenane were employed (Table 2) to calculate the ratios R_c(**A**:**B**) between the populations of **A** and **B**.

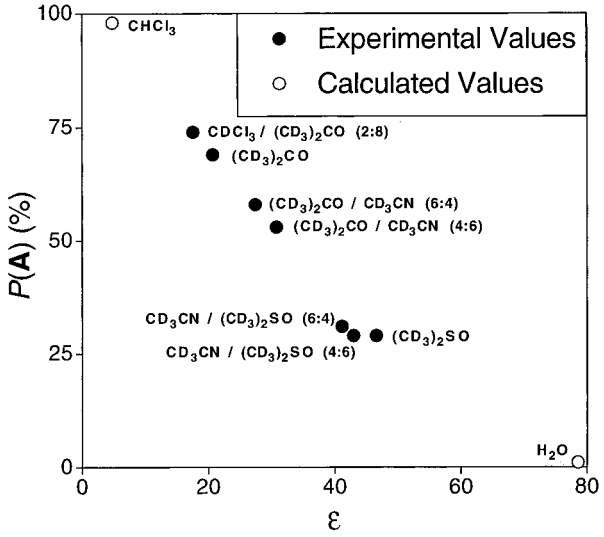

Figure 8. Correlation between the dielectric constant ϵ of the solvent and the experimental and calculated population P(**A**) of the translational isomer **A** of the [2]catenane **6**.

Table 1. Experimental and Calculated Data for the Complexes [7·13]−[12·13]

guest	$-\Delta G°$ [a] (kcal mol^{-1})	$-\Delta E$[b] (kcal mol^{-1})	$-E_p$[c] (kcal mol^{-1})	$-E_{HOMO}$[d] (eV)
7	4.6	20.1	20.5	7.7
8	4.1	18.1	21.9	8.2
9	*e*	11.6	16.9	7.6
10	*f*	16.1	−6.0	8.8
11	4.1	15.0	18.8	7.3
12	>5.0	22.1	22.6	7.2

[a] The experimental binding energies ($\Delta G°$) were measured in MeCN at 25 °C by employing hexafluorophosphate counterions with the tetracationic cyclophane **13** (refs 3b and 10c,g). [b] The ΔE values are the differences between the energies of the global minima of the complexes $E_{complex}$ and the energies of the global minima of the free host and guest E_{host} and E_{guest}, respectively [$\Delta E = E_{complex} - (E_{host} + E_{guest})$]. The global minima were found by performing a Monte Carlo conformational search on each species employing the AMBER* force field and the GB/SA solvation model for H_2O. [c] The HF/6-31G** electrostatic potential, E_p, measured at the surface of each aromatic unit. Dioxyarene and dithiaarene derivatives bearing methoxy substituents instead of the polyether chains were employed as the model compounds. [d] The HF/6-31G** energy, E_{HOMO}, of the HOMO. Dioxyarene and dithiaarene derivatives bearing methoxy substituents instead of the polyether chains were employed as the model compounds. [e] Not determined. [f] No complex formation was detected (refs 10e,h).

The geometries adopted in the solid state by the [2]-catenanes **2**, **4**, and **5** and the complex [**7**·**13**] were determined[3b,10b,c,e,g,h] experimentally by single crystal X-ray analyses. In all three [2]catenanes, only the translational isomer **A** incorporating the 1,4-dioxybenzene unit inside the cavity of the tetracationic cyclophane

(16) Polister, P.; Murray, J. S. *Reviews in Computational Chemistry*; Lipkowits, K. B., Boyd, D. B., Eds.; VCH: New York, 1991; Vol. 2, Chapter 7.

(17) The tetracationic cyclophane component was removed from the global minima of the complexes obtained from the Monte Carlo conformational searches. Similarly, the polyether substituents, attached to the aromatic units of the guests, were replaced by methoxy groups without modifying the dihedral angles around the Ar—O bonds. The resulting compounds were subjected individually to single point ab initio calculations performed at the HF/6-31G** level employing the program Spartan 4.1.

(18) Spartan V 4.1, Wavefunction, Inc., 18401 Von Karman Ave., Irvine CA 92715.

(19) The two translational isomers of each [2]catenane were constructed within the input mode of Macromodel 5.0, and their geometries were optimized by energy minimization, performed employing the PRCG method in conjunction with the AMBER* force field and the GB/SA solvation model for H_2O. The resulting structures were subjected individually to Monte Carlo conformational searches performed employing the default settings of Macromodel 5.0 in conjunction with the AMBER* force field and the GB/SA solvation model for either H_2O or $CHCl_3$.

Table 2. Experimental and Calculated Data Associated with the Translational Isomers A and B of the [2]Catenanes 2−6

		H_2O[b]					$CHCl_3$[c]				
[2]catenane	R_e(**A**:**B**)[a]	E(**A**)[d] (kcal mol^{-1})	E(**B**)[d] (kcal mol^{-1})	R_c(**A**:**B**)[e]	E_s(A)[f] (kcal mol^{-1})	E_s(**B**)[f] (kcal mol^{-1})	E(**A**)[d] (kcal mol^{-1})	E(**B**)[d] (kcal mol^{-1})	R_c(**A**:**B**)[e]	E_s(**A**)[f] (kcal mol^{-1})	E_s(**B**)[f] (kcal mol^{-1})
2	98:2	−122.9	−119.3	100:0	−420.7	−419.3	3.4	10.2	100:0	−294.4	−289.8
3	100:0	−112.6	−110.1	100:0	−174.3	−175.4	3.8	−40.1	0:100	−57.9	−105.4
4	100:0	−96.5	−92.1	100:0	−170.3	−165.2	32.9	35.3	99:1	−40.9	−37.8
5	30:70	−96.5	−98.4	2:98	−425.5	−427.9	20.3	−9.8	0:100	−308.7	−339.3
6	30:70 (70:30)[g]	−119.7	−121.7	1:99	−189.1	−189.7	5.2	7.0	98:2	−64.2	−61.0

[a] The experimental ratios R_e(**A**:**B**) between the translational isomers **A** and **B** of each [2]catenane were determined by ^{1}H NMR spectroscopy in $(CD_3)_2CO$ at 273 K in the case of **2**−**4**, in CD_3CN at 243 K in the case of **5**, and in $(CD_3)_2SO$ at 233 K in the case of **6** employing hexafluorophosphate counterions with the tetracationic [2]catenanes (refs 10a−c,e,g,h). [b] Data derived by performing Monte Carlo conformational searches on each isomer by employing the AMBER* force field and the GB/SA solvation model for H_2O. [c] Data derived by performing Monte Carlo conformational searches on each isomer by employing the AMBER* force field and the GB/SA solvation model for $CHCl_3$. [d] Energies of the global minima found for the translational isomers **A** and **B**. [e] Calculated ratios between the translational isomers of each [2]catenane derived employing the eq 1, where R is the gas constant and T is the temperature. The value of T at which the experimental populations were determined was employed in eq 1. [f] The solvation energies E_s(**A**) and E_s(**B**) of the translational isomers **A** and **B**, respectively, of each [2]catenane in H_2O and in $CHCl_3$ were calculated as the differences between the values of E(**A**) and E(**B**) calculated in the solvent and those calculated in the gas phase ($E_s = E_{solvent} - E_{gas}$). [g] The ratio in parentheses was determined in $(CD_3)_2CO$ at 233 K.

$$R_c(\mathbf{A}:\mathbf{B}) = e^{-\frac{E(\mathbf{A}) - E(\mathbf{B})}{RT}} \quad (1)$$

Table 3. Distances[a] (Å) and Angles[a] (deg) Characterizing the Geometries of the Translational Isomers A of the [2]Catenanes 2, 4, and 5 and of the Complex [7·13].

compd		θ_i	θ_a	τ	$Z_i\cdots Z_a$	$Y\cdots Y'$	$Z_a\cdots X_i$	$Z_i\cdots X_i$	$Z_i\cdots X_a$	$H\cdots Y$	XHY	$H'\cdots Y'$	H′XY′
2A	exptl[b]	10	5	46	6.97	10.06	3.52	3.46	4.15	2.59	160	2.70	158
	calcd[c]	18	30	51	6.88	10.29	3.53	3.35	4.02	2.86	153	2.73	157
4A	exptl[b]	12	1	46	6.98	10.23	3.51	3.47	4.01	2.73	160	2.74	159
	calcd[c]	9	29	44	6.86	10.29	3.52	3.34	3.31	2.69	162	2.83	156
5A	exptl[b]	10	12	44	6.81	10.30	3.46	3.39	3.44	2.87	155	2.62	168
	calcd[c]	16	31	46	6.96	10.21	3.55	3.42	3.36	2.65	166	2.76	156
[**7·13**]	exptl[b]	20	20	51	7.25	10.08	3.62	3.62		2.63	164	2.63	164
	calcd[c]	27	24	43	6.96	10.26	3.52	3.45		2.71	157	2.81	158

[a] The distances and angles indicated in the table are illustrated in the diagrams **I**, **II**, and **III**. The subscripts a and i stand for alongside and inside, respectively. [b] Determined by single-crystal X-ray analyses (refs 3b and 10b,c,e,g,h). [c] Derived from the analysis of the global minimum obtained from a Monte Carlo conformational search performed employing the AMBER* force field and the GB/SA solvation model for H_2O.

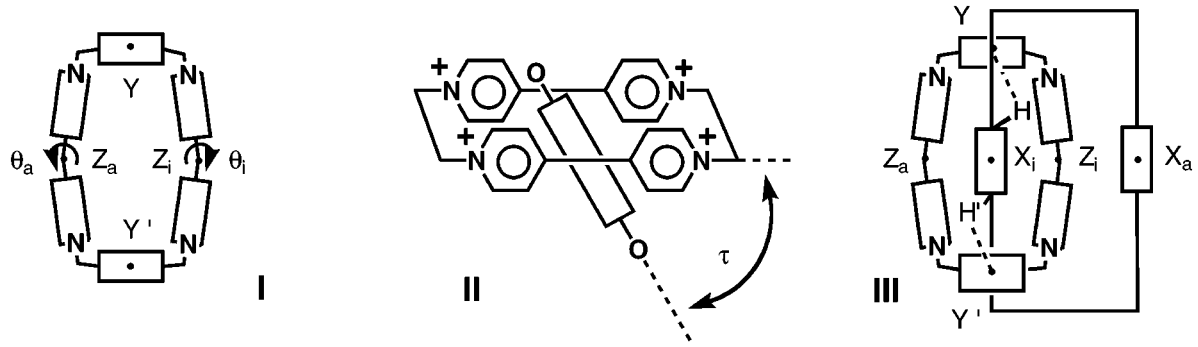

is observed in the solid state. To test the ability of the AMBER* force field to reproduce the geometries and the conformational energies of the [2]catenanes and of the complexes, the global minima found for the [2]catenanes **2**, **4**, and **5** and for the complex [**7·13**] were compared (Table 3 and Figures 5 and 6) with those of the solid state structures. Indeed, the calculated and experimental structures are remarkably similar. The only significant differences are the "bowing" angle θ_a of the "alongside" bipyridinium unit and the orientation of the dioxyarene unit residing "alongside" the tetracationic cyclophane in the [2]catenanes. These minor differences can probably be ascribed to crystal packing forces in the solid state.

Model Complexes. Comparison of the ΔE values listed in Table 1 shows that the complex formed (Figure 4) by the 1,4-dioxybenzene-based guest **7** and the host **13** is more stable than those formed by the guests **8**−**11**, but is less stable than the one formed by the 1,5-dioxynaphthalene-based guest **12**, in agreement with the experimental binding energies $\Delta G°$.[3b,10a,c,e−h] Interestingly, with the exception of the 1,4-dioxytetrafluorobenzene unit,[20] a linear correlation (Figure 7) is observed[21] between the calculated energy differences ΔE associated with the complexes and the electrostatic potential E_p of the corresponding model compounds: *the more negative the electrostatic potential, the stronger the calculated binding energy*. By contrast, no correlation is observed between the same energy differences ΔE and the HOMO

(20) Experimental binding studies revealed that the 1,4-dioxytetrafluorobenzene-based guest **10** is not bound (refs 10e,h) by the tetracationic cyclophane **13** in agreement with the high value calculated for the corresponding electrostatic potential E_p. Thus, the ΔE value associated with the complex [**10·13**], and derived from the molecular mechanics calculations, is significantly over estimated.

energies, E_{HOMO}, of the corresponding model compounds. Thus, even although strong charge-transfer bands are observed[3b,10a,c,e−h] experimentally in the visible spectra of the complexes, the binding event is governed by electrostatic, rather than by charge-transfer interactions.[21]

[2]Catenanes. In all [2]catenanes **2**−**6**, the ratios R_c(**A**:**B**) (Table 2) calculated with the GB/SA solvation model for H_2O are in very good agreement with the experimental ratios R_e(**A**:**B**) determined[10a−c,e,g,h] by ^{1}H NMR spectroscopy in high polarity solvents. In **2**, **4**, and **5**, the R_c(**A**:**B**) values calculated with the GB/SA solvation model for $CHCl_3$ are almost unchanged from those calculated for H_2O. In **3** and **6**, however, inversion of the ratios R_c(**A**:**B**) is observed on going from the solvation model for H_2O to that for $CHCl_3$. The solvent dependence of the ratio between the translational isomers **A** and **B** of **3** has not been investigated experimentally,[10g] but the inversion of the experimental ratio R_e(**A**:**B**) of **6** has been observed;[10a] the R_e(**A**:**B**) value varies from 30:70 in $(CD_3)_2$SO to 70:30 in $(CD_3)_2CO$. The plot of the experimental and calculated populations P(**A**) of the translational isomer **A** of **6** against the values of the dielectric constant of the media reveals (Figure 8) that, indeed, the calculated P(**A**) values follow the correlation observed for the experimental values.

The trend observed for the ΔE values (Table 1) of the model complexes [**7**·**13**]−[**12**·**13**], which is a reflection of the E_p values of their guests, is consistent with the experimental ratios R_e(**A**:**B**) and with the ratios R_c(**A**:**B**) calculated with the GB/SA solvation model for H_2O. The [2]catenane **5** is an exception: here, the 1,5-dithiaarene unit is located "inside" in preference to the 1,4-dioxybenzene unit. This anomaly, together with the solvent dependence of the R_c(**A**:**B**) values of **3** and **6**, can be explained by examining the values of the solvation energies E_s(**A**) and E_s(**B**) (Table 2) calculated for the translational isomers **A** and **B**, respectively, of each [2]catenane. In **5**, the translational isomer **B**, bearing the 1,5-dithiaarene unit "inside", is the more stable both in H_2O and $CHCl_3$. This selectivity contrasts with the ΔE and E_p values of the corresponding model compounds and is determined by the fact that the isomer **B** is more favorably solvated than **A**. In **3**, the difference between the E_p values of the two π-electron rich units contrasts with the difference between the solvation energies E_s(**A**) and E_s(**B**). In H_2O, however, a small difference in the solvation energies is observed and the electrostatic effects are dominant, driving the isomerism exclusively to **A**. In $CHCl_3$, the difference between E_s(**A**) and E_s(**B**) becomes dominant, leading exclusively to the isomer **B**. In **6**, a small difference between the E_p values of the two π-electron rich aromatic units is observed and the selectivity is controlled by the solvation energies. The difference between E_s(**A**) and E_s(**B**) varies from a positive to a negative value on going from H_2O to $CHCl_3$, causing the ratio between the translational isomers to reverse. These results suggest strongly that the translational isomerism is controlled (i) by the electrostatic effects which govern the $\pi-\pi$ stacking interactions between the "inside" π-electron rich unit and the sandwiching bipyridinium recognition sites and (ii) by the solvation energies of the two translational isomers. In **2** and **4**, these two factors are cooperative, and in **5**, the difference between the solvation energies is predominant, while in **3** and **6**, a subtle balance between the two factors drives the equilibrium between translational isomers in the direction of one or the other of the isomers.

Conclusions

The trend in the calculated energy differences ΔE between the energy of the global minimum of each complex and the sum of the energies of the global minima of its two separate host and guest components is in agreement with the trend shown by the experimental binding energies. The ΔE values can be correlated with the electrostatic potentials of the π-electron rich guests but not with their HOMO energies; *the binding event is dominated by electrostatic, rather than by charge-transfer, interactions*. An estimate of the equilibrium ratio between the translational isomers of each [2]catenane revealed that, in all cases, the major isomer observed experimentally corresponds to the one predicted by calculation. However, switching from H_2O to $CHCl_3$ inverts the equilibrium ratios between the translational isomers for two out of the five [2]catenanes. This prediction agrees with the experimental observations. Indeed, both calculated and experimental ratios can be correlated with the dielectric constant of the solvent. *The factors governing the translational isomerism are (i) the differences between the solvation energies of the two translational isomers and (ii) the differences between the binding energies of the corresponding supramolecular complexes which are controlled by electrostatic interactions.* It is the fine balance between these two factors that controls the relative populations of the translational isomers observed in solution. Computational methods are demonstrated to be a powerful tool for the analyses and prediction of complex molecular structures and their stabilities.

Acknowledgment. This research was supported by the Engineering and Physical Sciences Research Council in the U.K. and by the National Institute of General Medical Sciences, National Institutes of Health in the U.S.A.

JO980543F

(21) A similar result was observed for the binding of metal cations by aromatic compounds, see: (a) Mecozzi, S.; West, A. P.; Dougherty, D. A. *J. Am. Chem. Soc.* **1996**, *118*, 2307−2308. (b) Dougherty, D. A. *Science* **1996**, *271*, 163−168. (c) Ma, J. C.; Dougherty, D. A. *Chem. Rev.* **1997**, *97*, 1303−1324.